Sedimentary opal records in the eastern equatorial Pacific: It is not all about leakage

Nathalie Dubois,[1] Markus Kienast,[1] Stephanie Kienast,[1] Stephen E. Calvert,[2] Roger François,[2] and Robert F. Anderson[3]

Received 8 March 2010; revised 3 August 2010; accepted 10 September 2010; published 2 December 2010.

[1] The clear predictions of the silicic acid leakage hypothesis (SALH) resulted in a number of studies of downcore opal records from the tropical Pacific. The original SALH predicts that unused silicic acid, due to Fe-driven changes in Si versus N limitation, escaped from the glacial Southern Ocean to equatorial upwelling regimes where it enhanced diatom productivity, thereby decreasing coccolith growth and lowering atmospheric CO_2. In contrast to SALH predictions, however, sedimentary records from the eastern equatorial Pacific (EEP) do not show enhanced opal burial during the Last Glacial Maximum (LGM) but higher rates of opal burial during the deglaciation and marine isotopic stage 3 (MIS3). The peak in opal productivity during the deglaciation has been attributed to increased supply of nutrient-rich waters driven by stronger upwelling of deep water in the Southern Ocean at the end of last glacial period. The large peak in opal burial observed in a number of EEP cores during MIS3 was interpreted as evidence for Si leakage when Southern Ocean diatom productivity was limited by both low dust flux and extended sea ice. On the other hand, the paradoxical LGM decline in opal accumulation in the EEP was explained by enhanced dust input that lowered the diatom Si:C uptake ratio. Here we use a combination of molecular fingerprints of algal productivity and radioisotope tracers of sedimentation to revisit opal burial in the EEP, in particular during the MIS3 "opal peak." An increase in algal productivity is not supported by the sedimentary concentration of brassicasterol, an organic molecule commonly found in diatoms, or by the ratio of $(^{231}Pa/^{230}Th)_{xs,0}$, a proxy for opal export production. We therefore conclude that the large peak in opal burial during MIS3 reflects enhanced preservation of diatoms. Building on mechanisms invoked in previous studies, we hypothesize that opal burial in the EEP is controlled both by the physiological response of diatoms to low-latitude Fe inputs and by the high-latitude processes leading to silicic acid leakage.

Citation: Dubois, N., M. Kienast, S. Kienast, S. E. Calvert, R. François, and R. F. Anderson (2010), Sedimentary opal records in the eastern equatorial Pacific: It is not all about leakage, *Global Biogeochem. Cycles*, *24*, GB4020, doi:10.1029/2010GB003821.

1. Introduction

[2] A number of downcore opal records have been recently generated in the equatorial Pacific to test the Silicic Acid Leakage Hypothesis (SALH) [*Pichat et al.*, 2004; *Bradtmiller et al.*, 2006; *Kienast et al.*, 2006, *Richaud et al.*, 2007]. The SALH is built on the "silica hypothesis" erected independently by *Nozaki and Oba* [1995] and *Harrison* [2000], who proposed an increase in diatom production triggered by increased flux of dissolved silicon to the ocean released from a higher atmospheric dust input to account for the large and regular atmospheric CO_2 decreases during glacial periods. *Nozaki and Yamamoto* [2001] further suggested that the higher silicon and iron supply from higher atmospheric dust input to the sub-Antarctic zone could have caused a change from the modern dominance of carbonate-secreting plankton to diatom production, which preferentially utilized available nitrate, thereby out-competing coccolith production and increasing seawater alkalinity, leading to a lowering of atmospheric CO_2. *Brzezinski et al.* [2002] suggested that there was a switch between nitrate and silicic acid depletion in the Southern Ocean between Holocene and glacial periods due to increased supply of Fe to high southern latitudes, which lowers the silicic acid:nitrate uptake ratio of the resident

[1]Department of Oceanography, Dalhousie University, Halifax, Nova Scotia, Canada.
[2]Department of Earth and Ocean Sciences, University of British Columbia, Vancouver, British Columbia, Canada.
[3]Lamont-Doherty Earth Observatory, Earth Institute at Columbia University, Palisades, New York, USA.

0886-6236/10/2010GB003821

diatom population [*Franck et al.*, 2005]. *Matsumoto et al.* [2002a] extended this concept by erecting the SALH, which predicts that during glacial periods the excess silicic acid ($Si(OH)_4$) was transported from the Southern Ocean to lower latitudes within Subantarctic Mode Waters (SAMW). *Chase et al.* [2003] subsequently suggested that increased sea ice cover rather than increased Fe supply was the prime factor responsible for reduced Si utilization in glacial Antarctic surface waters. Sedimentary records of opal burial and nutrient utilization ($\delta^{30}Si$, $\delta^{15}N$) from the Southern Ocean are in agreement with the SALH, regardless of the cause for reduced Si consumption south of the Polar Front [*Chase et al.*, 2003; *Crosta et al.*, 2005; *Beucher et al.*, 2007].

[3] *Sarmiento et al.* [2004] suggested that the greatest increase in low-latitude opal burial should be observed in the eastern equatorial Pacific (EEP), as this is where the strongest surface signal of Southern Ocean waters is found today [*Toggweiler et al.*, 1991]. However, with the exception of a prominent peak in opal burial during marine isotopic stage 3 (MIS3) [*Kienast et al.*, 2006], downcore records of opal flux from the tropical Pacific are not consistent with the SALH and show, in fact, lower opal accumulation during glacial stage 2 [e.g., *Bradtmiller et al.*, 2006]. Subsequently, *Crosta et al.* [2007] invoked variations in the formation rate of Southern Ocean intermediate water as the main control on silicic acid leakage to the lower latitudes, and *Matsumoto and Sarmiento* [2008] pointed out that the key to SALH is the dominance of diatoms over coccolithophorids in low-latitude regions not the magnitude of diatom production per se.

[4] The fact that opal accumulation beneath low-latitude upwelling systems in the Pacific was lowest during glacial periods, when the potential for Si leakage from the Southern Ocean was greatest, raises questions not only about the sedimentary record of increased silicic acid supply to the low latitudes, but also more generally about the fidelity of a downcore opal record as a proxy for past changes in photic zone processes. The distribution of opal in surface sediments of the World ocean is clearly related on a whole ocean scale to the spatial distribution of surface water productivity [*Leinen et al.*, 1986], and downcore records of biogenic opal content have often been used to infer past changes in productivity at a given core site [e.g., *Charles et al.*, 1991; *Wefer et al.*, 1999; *Ragueneau et al.*, 2000]. However, most of the opal produced in the photic zone is rapidly regenerated within the water column [*Gilbert and Allen*, 1943], with only about 3% of the global opal production being finally buried [*Nelson et al.*, 1995], so that patterns of opal settling fluxes are not necessarily reflected in the bottom sediment [*Sancetta*, 1992; *Archer et al.*, 1993; *Romero et al.*, 1999]. In addition, downcore opal records can show little relationship between inferred productivity and organic matter accumulation [*Lange and Berger*, 1993; *Schneider et al.*, 1997]. Consequently, interpreting sedimentary opal records is not straightforward. The amount of opal buried at a given site depends not only on productivity in the surface ocean, but also on opal dissolution in the water column and in sediments, and on the lateral transport of sediments on the seafloor, all of which potentially change through time [*Bradtmiller et al.*, 2009].

[5] Here we investigate further the prominent peak in opal burial observed in EEP sediments during MIS3 (~35–60 kyr B.P.) [*Boyle*, 1983; *Kienast et al.*, 2006]. *Kienast et al.* [2006] suggested that the presence of this peak in the tropical Pacific corroborates the leakage mechanism postulated by the SALH, since it coincides with low opal fluxes in sedimentary records from the sub-Antarctic zone. But this large opal deposition event is not associated with an atmospheric CO_2 minimum as implied by the SALH. We therefore use a combination of molecular fingerprints of algal productivity and radioisotope tracers of sedimentation to discriminate between changes in diatom productivity and possible changes in opal preservation as the cause of enhanced opal burial.

2. Silica Supply and Opal Burial in the EEP

[6] The upwelling area in the EEP is a HNLC (high nitrate, low chlorophyll) region due to the presence of unutilized nitrate (NO_3^-) in the surface waters but low chlorophyll concentration [e.g., *Minas et al.*, 1986; *Dugdale and Wilkerson*, 1998]. The lack of Fe from atmospheric dust input was proposed initially as a cause of the incomplete utilization of nitrate (NO_3^-) by phytoplankton [e.g., *Chavez et al.*, 1990]. However, *Ku et al.* [1995], using ^{228}Ra determinations to derive nutrient fluxes in the equatorial Pacific, showed that upwelled $Si(OH)_4$ is limiting for diatom growth and the equatorial upwelling system has subsequently been designated more accurately as a low silicate-HNLC (LSiHNLC) system [*Dugdale et al.*, 1995]. Confirmation of equatorial $Si(OH)_4$ limitation was later obtained from ^{32}Si uptake experiments [*Leynaert et al.*, 2001].

[7] The primary source of nutrients for the modern EEP upwelling ecosystem is the Equatorial Undercurrent (EUC), which forms at the western end of the equator where waters from the Northern and Southern Hemispheres meet [*Dugdale et al.*, 2002]. Although the contribution of water volume to the EUC is roughly equal between the Northern and Southern Hemispheres, the southern sourced waters are depleted in $Si(OH)_4$ relative to NO_3^- [*Sarmiento et al.*, 2004], which contributes to the LSiHNLC character of the EEP. In the Southern Ocean, waters strongly deficient in $Si(OH)_4$ compared to NO_3^- are formed during the Austral summer productivity season [*Hiscock et al.*, 2003] and advected northward as SAMW [*Toggweiler et al.*, 1991; *Dugdale et al.*, 2002]. As a result, changes in $Si(OH)_4$ in the Southern Ocean should affect equatorial $Si(OH)_4$ supply and diatom production.

[8] Amorphous silica, or opal, is produced by diatoms, silicoflagellates and radiolarians in the upper ocean. In the central equatorial Pacific (1°N, 139°W), *Murray* [1987] determined that 75%–80% of the total opal flux was of diatom origin. Because the ocean is everywhere undersaturated with respect to biogenic opal [e.g., *Stumm and Morgan*, 1981], dissolution occurs at all depths in the water column and continues during burial until either the interstitial waters become saturated or altered chemical composition of the particle surfaces prevents further disso-

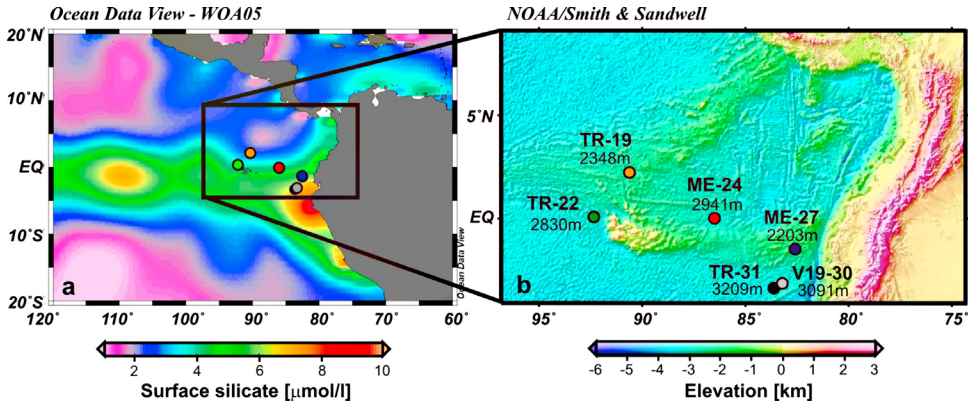

Figure 1. (a) Core locations plotted on a map showing mean annual silicate distribution in surface waters from the World Ocean Atlas 2005 [*Garcia et al.*, 2006]. For latitude/longitude information, see text. (b) Core locations plotted on seafloor topography from *Smith and Sandwell* [1997]. Water depths at core locations are indicated below the core names.

lution [e.g., *Kamatani et al.*, 1988]. The accumulation of opal in marine sediments seems to result primarily from those conditions that enhance preservation of silica through the water column: shallow water depth, low SST, trace element incorporation into the frustules, rapid sinking rates and other biological factors (species composition, nutrient limitations) [*Ragueneau et al.*, 2000]. Indeed, diatom blooms are a main source of the opal preserved in sediments [*Nelson et al.*, 1995], since preservation and export are enhanced by the formation of diatom aggregates and the incorporation of opal into fecal pellets by grazers [e.g., *Tande and Slagstad*, 1985].

[9] Once on the seafloor, the opal raining from the surface can potentially be transported laterally. Earlier studies in the EEP have suggested that winnowing from the ridges into the basin is the dominant factor governing the sedimentary distribution of opal [*Moore et al.*, 1973]. The finest (e.g., diatoms) and lightest (e.g., radiolarian) particles are preferentially removed from the ridges, while coarser and heavier deposits (e.g., whole foraminifera) remain on the ridges [*Van Andel*, 1973]. This is reflected in the augmentation of the sedimentary section in many cores due to focusing, as shown by ^{230}Th normalization of the bulk sediment accumulation rate [*Kienast et al.*, 2007; *Winckler et al.*, 2008]. Therefore, the concentration of opal in the deep basins (and of calcite on the ridges) in the EEP is more closely related to topography than to productivity [*Moore et al.*, 1973]. *Kusch et al.* [2010] have shown that the focusing of sediment at some core sites in the EEP is due to the syndepositional accumulation of material that has not been significantly aged, indicating that short-distance bottom redistribution of material has inflated the sediment record but has not seriously biased it.

3. Materials and Methods

3.1. Core Material

[10] We present new records of opal concentration, ^{231}Pa/^{230}Th ratios, brassicasterol concentrations and ^{230}Th normalized fluxes of opal, bulk sediment, calcium carbonate and detrital material of four cores from the EEP covering the last 100 kyr, expanding two records (ME0005-24JC and ME0005-27JC) previously published by *Kienast et al.* [2007]. We combine these new data with two previously published opal flux records from the same area (TR163-19 and TR163-31P [*Kienast et al.*, 2006]). Figure 1a shows the core location on a map of present-day surface water silicate concentration, while Figure 1b gives the core locations on a topographic map.

[11] Core ME0005-24JC (0°01.302′N, 86°27.788′W; hereinafter abbreviated as ME-24) was recovered from an abyssal valley just to the north of the Carnegie Ridge in 2941 m water depth (wd). Core ME0005-27JC (1°51.201′S, 82°47.20′W, ME-27) was raised on the southern flank of the Carnegie Ridge in 2203 m wd, from a bench that gently slopes to the south, approximately 20 km south of the main scarp of the Carnegie Ridge. Further to the south, core TR163-31P (3°35′S, 83°57′W, TR-31) was recovered in 3205 m wd. Core V19-30 (3°23′S, 83°21′W) was recovered very close to TR-31, in 3091 m wd. Core TR163-22 (92°23.90′W, 0°30.90′N, TR-22) was recovered 200 km NW of the Galapagos Islands in 2830 m wd. Finally, core TR163-19P (90°57.10′W, 2°15.50′N, TR-19) was raised from 2348 m wd on the outer flank of the Cocos Ridge, which forms the western boundary of the Panama Basin.

[12] The age models for cores ME-24, TR-22 and V19-30 are adopted as previously published (ME-24 [*Lyle et al.*, 2005; A. Mix, unpublished data, 2006]; TR-22 [*Lea et al.*, 2006]; V19-30 [*Shackleton et al.*, 1983]). The age model for core ME-27 is adopted as published by [*Kienast et al.*, 2007] for the last 35 kyr, while the oldest part is based on benthic δ^{18}O stratigraphy (A. Mix, unpublished data, 2006).

3.2. Analytical Methods

[13] Biogenic opal (Siopal) in cores ME-24 (>35 kyr B.P.), ME-27 (>35 kyr B.P.), and TR-22 was determined at Dalhousie University by extraction of amorphous silica from 20 mg subsamples using a 2 M Na_2CO_3 solution at 85°C for 5 h [*Mortlock and Froelich*, 1989], followed by the

measurement of dissolved silica concentrations in the extract by molybdenum blue spectrophotometry. Biogenic opal in core V19-30 was determined at LDEO following a similar procedure, while the top parts (<35 kyr B.P.) of ME-24 and ME-27 were determined at UBC. Percent opal is calculated as 2.4 × % Siopal. Precision from duplicates was ±1%, and repeat analyses between UBC and Dalhousie agree to within ±1.5%. Biogenic opal values in cores TR-19 and TR-31 are taken from *Kienast et al.* [2006] and those of core V19-30 for the last 20 kyr B.P. are taken from *Bradtmiller et al.* [2006], where determinations were made using the same procedures.

[14] Changes in the relative concentration of brassicasterol in core ME-24 were determined by gas chromatography at Dalhousie University. Approximately 1 g of freeze-dried sediment was extracted using a Dionex Accelerated Solvent Extraction system (ASE200). These extracts were saponified using potassium hydroxide and purified through silica column chromatography. The purified extracts were then treated with bis(trimethylsilyl)trifluoroacetamide (BSTFA) to derive trimethyl silyl esters (TMS) before gas chromatographic analysis. Relative sterol distributions were determined by integration of the sterol peak area in the chromatogram, normalized to sample weight. We did not use recovery standards and thus the normalized brassicasterol chromatographic peak areas we report were not corrected for potential losses during the extraction process.

[15] Uranium (^{238}U), thorium (^{232}Th, ^{230}Th) and protactinium (^{231}Pa) concentrations were determined at the University of British Columbia (UBC), LDEO and the Woods Hole Oceanographic Institution (WHOI) by isotope dilution on an inductively coupled plasma mass spectrometer (ICP-MS) following total acid digestion of sediment samples equilibrated with ^{229}Th and ^{236}U spikes and anion resin column chemistry to separate the Pa and U/Th fraction. Details and principles of the procedure can be found in the work of *Choi et al.* [2001] and *Francois et al.* [2004]. Radioisotope data for cores TR-19 and TR31 are from *Kienast et al.* [2006], and those of core V19-30 for the last 20 kyr are from *Bradtmiller et al.* [2006]. Data for the last 35 kyr B.P. for cores ME-24 and ME-27 are from *Kienast et al.* [2007].

[16] Total carbon was determined by flash combustion gas chromatography with CHN elemental analyzers at Dalhousie (ME-24 > 35 kyr B.P.; ME-27 > 35 kyr B.P.; TR-22), UBC (ME-24 < 35 kyr B.P.; ME-27 < 35 kyr B.P.; TR-19; TR-31) and LDEO (V19-30). Relative standard deviation (R.S.D.) were always <±2% (1σ) based on several standards analyzed along with the samples. Inorganic carbon was determined directly by CO_2 evolution after HCl treatment of the sediment samples in a carbon dioxide coulometer with an analytical precision of ±2.3% (1 σ, R.S.D.). Organic carbon was estimated by subtracting inorganic from total carbon, with a combined analytical precision (as R.S.D.) of ±3%. $CaCO_3$ values were obtained from the coulometric CO_2 determinations assuming no other carbonate-bearing phase was present.

3.3. Approach

[17] Opal fluxes were calculated by normalizing to ^{230}Th to correct for lateral redistribution of sediments by deep-sea currents [*Francois et al.*, 2004]. Setting the vertical flux of ^{230}Th to the seafloor equal to its known production rate, fluxes of preserved material can be calculated as: ${}^{pr}F_v = C \times \beta \times z/{}^{230}Th_{xs,0}$ where F is the flux of the sedimentary constituent of interest, C is the concentration of that constituent in bulk sediment (i.e., opal), $\beta \times z$ is equal to the production rate of ^{230}Th in the water column (z is the depth of the water column (cm) and $\beta = 2.63 \times 10^{-5}$ dpm cm^{-3} ka^{-1}), and ${}^{230}Th_{xs,0}$ is equal to the decay-corrected concentration of ^{230}Th in the sample (dpm/g) in excess of that supported by its parent, ^{234}U.

[18] Like ^{230}Th, ^{231}Pa is produced by radioactive decay of dissolved uranium (^{235}U), and is removed from seawater by scavenging to particles. Because of its particular affinity for sorption to opal over other particle composition, ^{231}Pa has been recently proposed as a tracer of opal flux [*Dezileau et al.*, 2003; *Bradtmiller et al.*, 2006, 2007; *Anderson et al.*, 2009]. Less particle reactive than thorium, protactinium has a longer residence time in the ocean and tends to be removed by scavenging in regions of high particle flux, preferentially by opal [*Anderson et al.*, 1983, 1990]. Although the particle flux has some influence on the $(^{231}Pa/^{230}Th)_{xs,0}$ ratio of sediments (also decay corrected, and in excess of that supported by the respective parent isotopes), the strong correlation between $(^{231}Pa/^{230}Th)_{xs,0}$ ratios and opal fluxes in many sediment records supports the view that opal flux is the primary variable determining the sedimentary $(^{231}Pa/^{230}Th)_{xs,0}$ ratio [*Dezileau et al.*, 2003; *Bradtmiller et al.*, 2006, 2007; *Anderson et al.*, 2009].

[19] Brassicasterol (24-methylcholesta-5,22E-dien-3β-ol) has been used as a molecular indicator for the presence of diatoms based on the observation that it can account for over 90% of the total sterols in most diatoms [*Volkman*, 1986], and downcore variations in brassicasterol concentration have been previously interpreted as indicating production changes related to diatom abundances [e.g., *Schubert et al.*, 1998; *Calvo et al.*, 2004; *Higginson and Altabet*, 2004; *Sachs and Anderson*, 2005]. As an organic marker, brassicasterol is affected by different preservational controls than opal and Pa/Th, therefore providing an independent line of evidence for changes in diatom production. We note however that a more recent study suggests that brassicasterol is only the fifth most common sterol in diatoms and that high relative concentrations of brassicasterol appear to be restricted to pennate diatoms [*Rampen et al.*, 2010]. In addition, most of the major sterols have also been reported in other groups of algae like *Haptophyceae* and *Cryptophyceae* [*Conte et al.*, 1994; *Volkman*, 2003]. Thus, we do not use brassicasterol as an indicator for diatom presence per se, since we have observations of diatoms from smear slides (see below). Acknowledging the ambiguity of this proxy, we use it as a corroborating line of evidence only.

4. Results

4.1. Opal Percent

[20] Over the last 100 kyr B.P., sedimentary records of opal percentage covary in a significant number of cores from the EEP (Figure 2a). The new record generated here

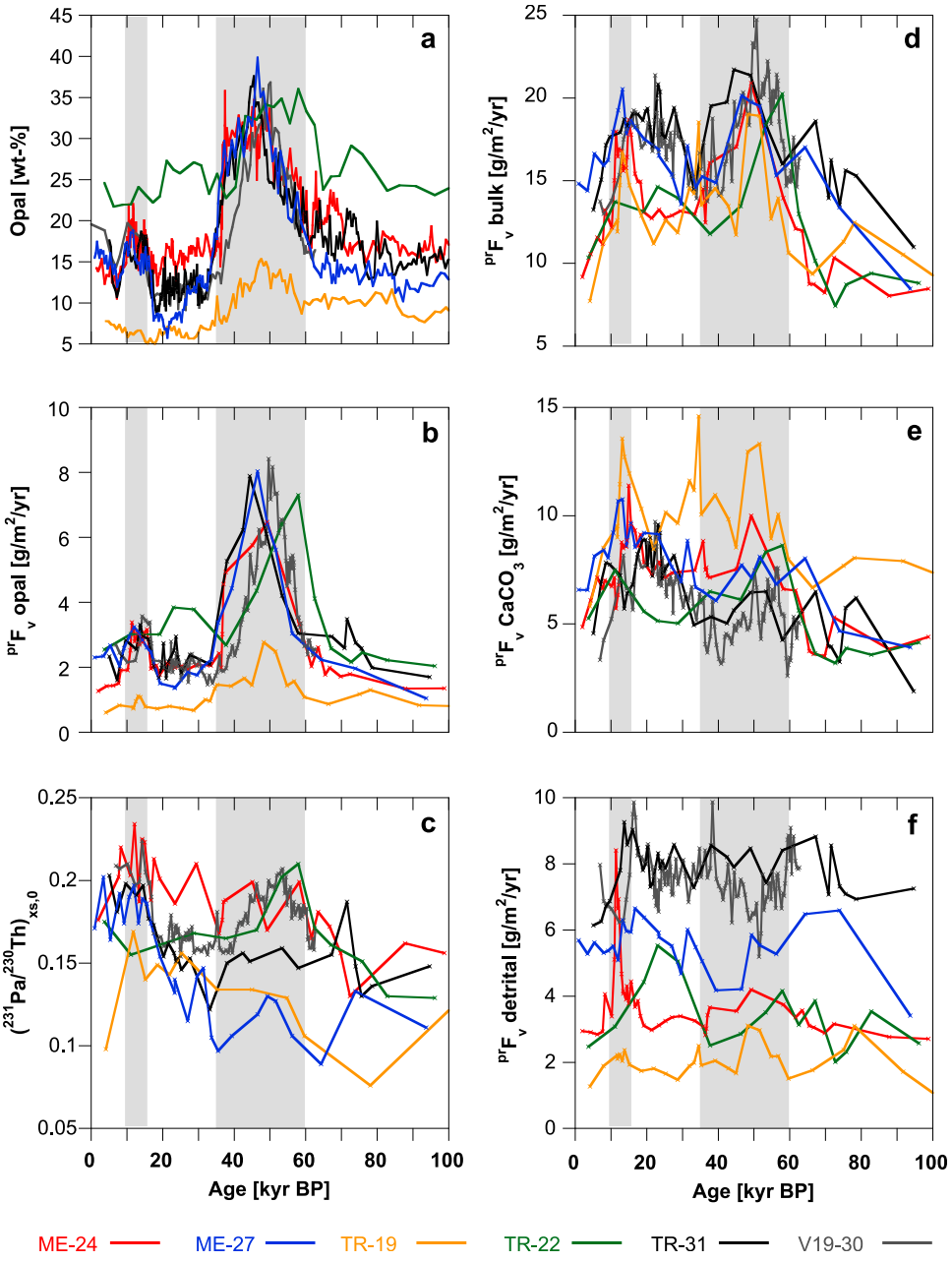

Figure 2. Productivity proxies plotted against age in six eastern equatorial Pacific cores used in this study (see text and Figure 1 for locations). (a) Opal percentage. (b) Preserved vertical opal fluxes. (c) The $(^{231}Pa/^{230}Th)_{xs,0}$ ratios. (d) Preserved vertical bulk fluxes. (e) Preserved vertical $CaCO_3$ fluxes. (f) Preserved vertical detrital fluxes. Preserved vertical fluxes ($^{pr}F_v$) are estimated using the ^{230}Th normalization procedure (see text [*Francois et al.*, 2004]). Cores are distinguished by the same color as in Figure 1. The "deglaciation peak" and "opal peak" intervals discussed in the text are indicated by gray shadings.

for ME-24 agrees well with the lower-resolution record previously published by *Lyle et al.* [2005]. All records show an important peak from ~35–60 kyr B.P. The increase in opal content is more gradual than the decrease, which occurs in less than 5 kyr. In addition, a deglacial peak is clearly present in cores ME-24, ME-27, TR-31 and V19-30, and the higher-resolution records reveal rapid fluctuations of 2–5 kyr and up to 10% opal that are superimposed on the longer-term record (Figure 2a).

[21] The absolute value of opal content depends on water depth (as it affects the $CaCO_3$ content), topographic location (due to winnowing or focusing), and the surface productivity at the core location. The opal content in TR-19 remains lower than in the other records throughout the last

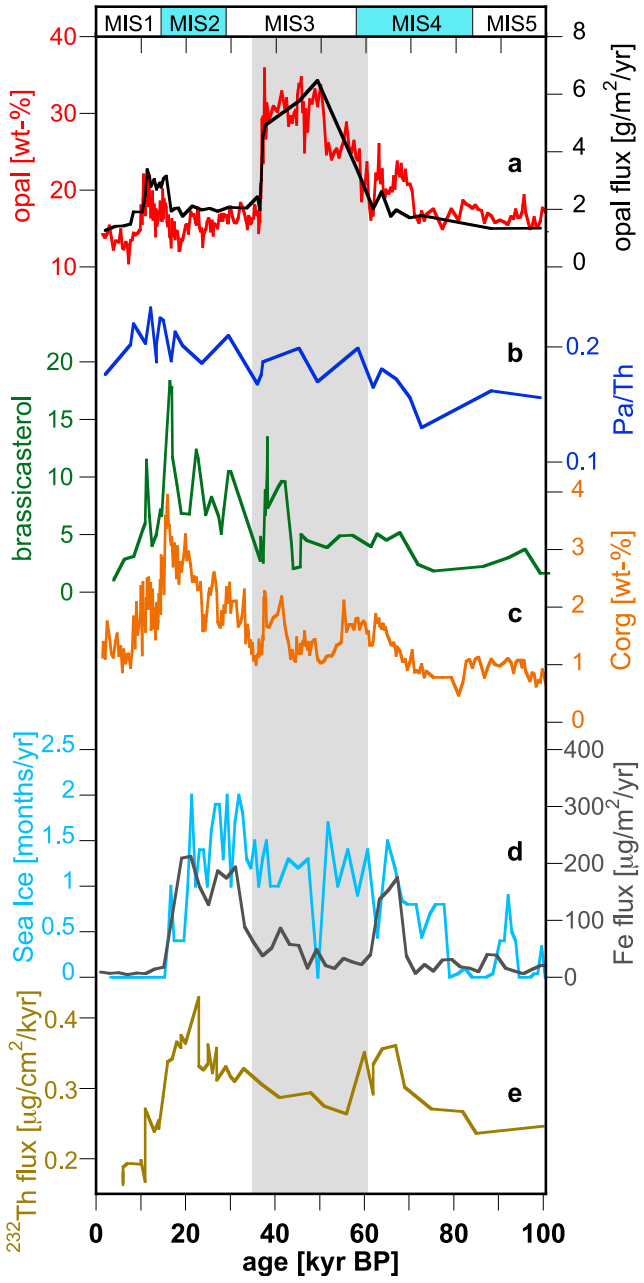

Figure 3. Multiproxy record of core ME-24 from the EEP compared to published records of dust flux from the Antarctic Ice Sheet and the central equatorial Pacific. (a) Opal percentage and ^{230}Th-normalized opal flux from ME-24. (b) Downcore $(^{231}Pa/^{230}Th)_{xs,0}$ ratios from ME-24. (c) Relative chromatographic peak area of brassicasterol and organic carbon percentage in ME-24. (d) Iron (Fe) flux from the EPICA ice core [*Wolff et al.*, 2006] and sea ice cover [*Crosta et al.*, 2004]. (e) The ^{232}Th flux from core TTN013-PC72 in the central equatorial Pacific [*Winckler et al.*, 2008]. The opal peak interval (35–60 kyr B.P.) is highlighted in gray, and marine isotopic stages (MIS) are indicated at the top of the plot.

100 kyr (Figure 2a). Although one explanation could be winnowing of opal from the location of this core on the Cocos Ridge or higher accumulation of $CaCO_3$ at its lower water depth (2348 m), the higher opal content in ME-27, which is located at similar water depth on the Carnegie Ridge (Figure 1b) would rather suggest that a lower biological productivity at TR-19 is the main factor (140 gC/m^2/yr at TR-19 compared to 200 gC/m^2/yr at ME-27 [*Antoine et al.*, 1996]), considering its location at the northern boundary of the equatorial upwelling zone. In contrast, core TR-22 generally shows the highest opal concentrations, which could be due to its relatively deep location (2830 m) enhancing $CaCO_3$ dissolution, winnowing from the ridges, its location immediately below the equatorial upwelling zone, as well as its position farther away from the coast of South America, which leads to lower detrital input. The four remaining cores (ME-24, ME-27, TR-31 and V19-30) show somewhat similar opal values, in particular during the opal maxima in MIS1 and 3 (Figure 2a). The slight offset in the timing of both the MIS3 and millennial-scale opal peaks is probably due to small uncertainties in the age models. The largest differences in opal concentration between core sites are observed during MIS 2 and 4. The opal content of ME-27 is constantly about 5% lower than the three other cores, due to its shallower depth and higher $CaCO_3$ content. On the other hand, opal concentration of ME-24 is usually slightly higher, possibly due to its location in an abyssal valley favoring deposition of finer material winnowed from the ridges (Figure 1b).

[22] Smear slide observations (see Table S1) of selected samples show that diatom tests are the most abundant siliceous organisms in the studied interval, with only minor occurrences of Radiolaria and silicoflagellates.[1]

4.2. Total Burial Fluxes

[23] Downcore records of bulk sediment flux plotted against model age for each core can be seen in Figure 2d. Total preserved rain rates vary between 7 and 25 g/m^2/yr. The records are similar in the six cores, with minimum values during the Holocene, a deglacial peak, though more clearly defined in ME-24 and TR-19, maximum bulk fluxes around 50 kyr B.P., and a gradual decrease >50 kyr B.P. Both peaks around 15 and 50 kyr B.P. reach similar values, except in V19-30, TR-22 and TR-31 where the oldest peak is higher. On average, bulk fluxes appear to decrease with distance from the South American coast.

4.3. Preserved Opal Rain Rates

[24] Th-normalized opal fluxes show a consistent pattern of temporal variability (see Figure 2b). ME-24, ME-27, V19-30, TR-22 and TR-31 show very similar records, with a base value of ~2 g/m^2/yr. Core TR-19 records lower opal fluxes with a mean of ~1 g/m^2/yr. A deglacial maximum between 10 and 15 kyr B.P. is present in every core except TR-22, although more pronounced and lasting longer in ME-24, ME-27, V19-30 and TR-31. In those four cores,

[1]Auxiliary materials are available in the HTML. doi:10.1029/2010GB003821.

opal fluxes increase by more than 1 g/m^2/yr, while in TR-19, opal fluxes increase by ~0.3 g/m^2/yr between 13 and 17 kyr B.P. A major opal flux maximum is observed in every core during MIS3. During this peak, opal flux reaches 2.5 g/m^2/yr in TR-19, 6.5 g/m^2/yr in ME-24, 7.3 g/m^2/yr in TR-22, 7.9 g/m^2/yr in TR-31, 8.0 g/m^2/yr in ME-27 and 8.4 g/m^2/yr in V19-30. This geographic pattern reflects to a certain point the present-day distribution of silicic acid in EEP surface waters, with the highest values to the southeast of V19-30 and TR-31, decreasing toward ME-27, ME-24 and finally TR-19 (see Figure 1a).

4.4. The $(^{231}Pa/^{230}Th)_{xs,0}$ Ratio

[25] In all our cores, except TR-19, the $(^{231}Pa/^{230}Th)_{xs,0}$ activity ratio remains above the production rate ratio (0.093; Figure 2c). In TR-19, the $(^{231}Pa/^{230}Th)_{xs,0}$ record varies from 0.08 to 0.17, while in V19-30, TR-31, ME-24 and ME-27, it varies from ~0.10 to >0.20. Highest values are observed during the deglaciation (10–20 kyr B.P.), except in V19-30 and TR-22, where slightly higher values occur during the opal peak. Both ME-27 and TR-31 show a downcore decreasing trend from ~15 to 30 kyr B.P. TR-19 on the other hand still records high values, while in ME-24 the variability is too high to observe any conclusive trend (Figure 2c). During MIS3, slightly higher values are observed in ME-24, TR-31 and ME-27, but they do not reach the deglacial values as is the case in V19-30 and TR-22. Core TR-19 does not record any significant change. The discrepancy in Pa/Th ratios between neighboring cores V19-30 and TR-31 for the interval 40–60 kyr B.P. is anomalous, given the very similar opal content and opal fluxes. This disagreement is still under investigation.

4.5. Brassicasterol and Organic Carbon

[26] Downcore variations in the relative peak area of brassicasterol in ME-24 reveal slightly elevated values from 75 to 44 kyr B.P., a maximum between 37 and 42 kyr B.P. with abrupt transitions, and higher amplitude variability during the last 30 kyr (Figure 3c). The organic carbon (Corg) content shows a very similar pattern (see Figure 3c).

5. Discussion

[27] Our data show that deglacial and MIS3 peaks in opal content are common to cores recovered from a range of water depths and topographic settings in the EEP. These peaks are matched by maxima in opal burial fluxes. The $(^{231}Pa/^{230}Th)_{xs,0}$ activity ratio also has a deglacial maximum, and correlates significantly with opal burial fluxes during the Holocene [see also *Bradtmiller et al.*, 2006] and the deglaciation. The nature and the details of each of these relationships vary during different time intervals over the last 60 kyr. Here we present a further analysis and reevaluation of the processes that may have produced the two opal flux maxima over the last 60 kyr in the EEP.

5.1. Enhanced Productivity

[28] Following the commonly accepted interpretation of variations in opal burial, the large opal peak in MIS3 sediments from the EEP was initially interpreted as resulting from higher opal production based on higher Th-normalized opal flux (Figure 2b) [*Kienast et al.*, 2006]. The bulk sediment flux only shows a slight increase over that particular interval (see Figure 2d) and thus the opal content is the main driver of the peak in opal flux (since opal flux = opal percentage × bulk flux). As stated in the introduction, the opal content of sediments is influenced by production, dissolution and redistribution. Normalization of opal accumulation records using particle-reactive natural radionuclides may correct for sediment redistribution artifacts, but not for opal dissolution before it arrives at the seafloor or in the sediment [*De La Rocha et al.*, 1998]. In addition, higher opal productivity does not necessarily lead to higher preservation in the sediments. *Warnock et al.* [2007] observe that increased production causes rapid silica recycling in the photic zone and the production of thinner-walled frustules, resulting in enhanced water column dissolution. We present two lines of evidence that argue against a large increase in opal production as the cause of the MIS3 peak in opal burial.

[29] First, the brassicasterol record in ME-24 does not show an increase in relative concentration synchronous with the large opal peak (Figure 3c). Although we acknowledge the ambiguity of this indicator and the preliminary nature of our brassicasterol data (see methods), a substantial increase in diatom productivity during the MIS3 as suggested by the opal flux record should have left an imprint in the sterol record. The record of diatom sterols thus lends no support to a significant increase in diatom productivity during the opal peak. This discordance could be due to (1) an increase in the production of radial centric diatoms (in which brassicasterol is absent) and (2) the differential preservation of the organic molecule brassicasterol compared with diatomaceous opal. We note however that smear slide observations on samples of ME-24 do not reveal significant downcore changes in the diatom assemblage.

[30] A second argument against higher opal productivity is given by the downcore $(^{231}Pa/^{230}Th)_{xs,0}$ records. Nuclide ratios such as Pa/Th are not affected by remineralization of biogenic phases at the seabed. Therefore, the $(^{231}Pa/^{230}Th)_{xs,0}$ ratio documents past changes in opal export fluxes rather than preserved opal rain rates [*Dezileau et al.*, 2003]. A recent study by *Bradtmiller et al.* [2006] found a significant linear relationship (r^2 = 0.66) between opal flux and the $(^{231}Pa/^{230}Th)_{xs,0}$ ratio in Holocene sediments from the equatorial Pacific. The data presented here follow the same relationship (see Figure 4a), even improving the r^2 when combined with the data of *Bradtmiller et al.* [2006] (r^2 = 0.70). We show in Figure 4b that a similar linear correlation holds during the last 19 kyr B.P., an interval including the deglacial opal peak (r^2 = 0.70), and even during the Last Glacial Maximum (LGM) (19–23 kyr B.P.) although with a larger amount of scatter (r^2 = 0.47; Figure 4c). As shown in Figure 4e, the correlation between $(^{231}Pa/^{230}Th)_{xs,0}$ and total preserved sediment rain rates during the Holocene is weaker than with opal flux (r^2 = 0.41), supporting the view that opal flux is the primary variable determining sedimentary Pa/Th ratios in the EEP over the last 20 kyr.

[31] As observed previously by *Bradtmiller et al.* [2006], the $(^{231}Pa/^{230}Th)_{xs,0}$ ratios in EEP cores are maximal during

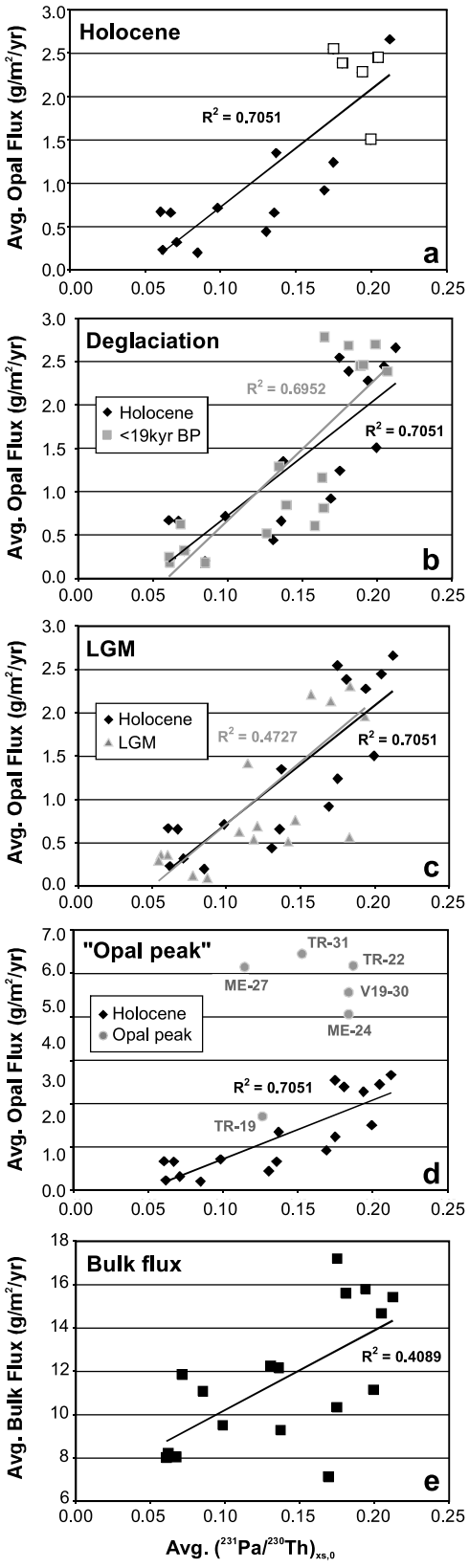

the deglaciation coeval with higher opal fluxes (see Figures 2b, 2c, 3a, and 3b). However, during the MIS3 (35–60 kyr B.P.), the $(^{231}Pa/^{230}Th)_{xs,0}$ ratios in cores ME-24, ME-27, TR-19 and TR-31 show only a slight increase, smaller than the deglaciation maxima, while values similar to or higher than the deglaciation are reached in core V19-30 and TR-22 (Figure 2c). Therefore, our radionuclide data are not consistent with a large increase in the production and settling of opal. This result is supported by the $(^{231}Pa/^{230}Th)_{xs,0}$ record from ODP Site 849, which also shows only a small increase during MIS3, lower than the deglacial increase [*Pichat et al.*, 2004]. These observations are supported by the poor relationship between the opal flux and the $(^{231}Pa/^{230}Th)_{xs,0}$ ratio during the MIS3 opal peak interval (Figure 4d).

[32] Three factors have the potential to decouple the downcore $(^{231}Pa/^{230}Th)_{xs,0}$ ratio from opal flux: (1) temporal variability in opal preservation; (2) temporal variability in the flux of $CaCO_3$ or detrital material, either of which could influence Pa/Th ratios [e.g., *Chase et al.*, 2002]; and (3) temporal variability in the dissolved Pa/Th ratio of deep waters [*Bradtmiller et al.*, 2007]. We favor the first explanation for the decoupling of the two signals over the interval of interest since there are large variations in the opal fluxes and there are no large-scale variations in the detrital or $CaCO_3$ fluxes (Figures 2e and 2f). Although we cannot rule out that changes in the dissolved Pa/Th ratio of bottom water contributed to the decoupling of opal flux and Pa/Th ratios during the opal peak interval, we assume this factor to be minimal. A significant reduction in bottom water Pa/Th ratios of the EEP would imply a dramatic slowdown of intermediate and deep-water circulation in this area. Alas, no studies to date have addressed the circulation of bottom water in the Eastern Pacific during the time interval of interest. However, for the LGM, a time of large-scale changes in circulation in the Atlantic, studies have shown

Figure 4. Correlation between ^{230}Th-normalized opal fluxes, bulk fluxes, and $^{231}Pa/^{230}Th$ ratios in the equatorial Pacific averaged over selected time intervals. (a) Correlation between average Holocene (0–10 kyr) opal fluxes and $^{231}Pa/^{230}Th$ values in each core. Black diamonds show data from *Bradtmiller et al.* [2006], and open squares correspond to data from this study. (b) Same correlation of the average values of the last 19 kyr B.P., shown by gray squares. Black diamonds show the Holocene averages. (c) Same correlation of the average values during the LGM (19–23 kyr B.P.), shown by gray triangles. Black diamonds show the Holocene averages. Note the almost identical linear relationship but larger scatter of LGM values as compared to the Holocene. (d) Correlation between opal fluxes and $^{231}Pa/^{230}Th$ values averaged over the "opal peak" interval (35–60 kyr B.P.) is shown by gray circles. Black diamonds show the Holocene averages, and black r^2 is based on Holocene data only. (e) Correlation between the bulk sediment flux and $^{231}Pa/^{230}Th$ values averaged over the Holocene (0–10 kyr). The *Bradtmiller et al.* [2006] data are merged with ours in Figures 4b, 4c, 4d, and 4e.

that Pacific deep-water circulation has remained similar to the present circulation [*Matsumoto and Lynch-Stieglitz*, 1999; *Matsumoto et al.*, 2002b].

[33] In light of these considerations, we propose that the higher opal percentages observed in sedimentary records from the EEP during MIS3 are not the result of enhanced opal export production. We are thus left with two other possible drivers: changes in the seafloor opal redistribution or dissolution of opal.

5.2. Opal Redistribution

[34] Exploring the discrepancies between two closely adjacent core sites, *Kienast et al.* [2007] stated that: "the preferential advection of a minor sediment constituent such as organic carbon or opal would not significantly affect the ^{230}Th-normalized flux of bulk sediment and major sediment constituents, but would increase the % Corg and % opal at the receiving site, resulting in higher ^{230}Th-normalized values of these constituents." Large-scale redistribution events in this region would be unlikely; a source for a large mass of redistributed opal has not been identified, all sedimentary records from the EEP reveal an increase in opal content during the same time period, and coring sites are located in diverse topographic settings (i.e., ridge, valley). Moreover, sea level fluctuations and shore line positions during MIS3 would not be conducive for remobilization of sediments on the continental shelves. Local contemporaneous redistribution of sedimentary constituents has occurred in the Panama Basin, as shown by insignificant radiocarbon age differences between organic carbon, planktonic foraminifera and alkenones in cores ME-24 and closely adjacent Y69-71P [*Kusch et al.*, 2010], demonstrating that the material that has inflated the bulk sediment accumulation rate over that supplied from the sea surface has not been preaged but has been moved syndepositionally to the core sites. This strongly implies that the downcore proxy record in this region of the EEP is a faithful record of paleoceanographic and sedimentary events despite clear evidence of sediment focusing [*Kienast et al.*, 2007].

5.3. Enhanced Preservation

[35] The fraction of deposited biogenous silica that is regenerated (dissolved) in modern sediments can be estimated from pore water dissolved silicon profiles, but this approach is not applicable to the sedimentary record. Indeed, no reliable methods are presently available by which such an estimate can be made [*Dezileau et al.*, 2003]. The only approach currently existing to estimate opal preservation and the effects of dissolution is to look at the diatom assemblage [e.g., *Pichon et al.*, 1992] or to assess the valve preservation of a robust species [*Warnock et al.*, 2007].

[36] At depths between 2200 and 3200 m, all the core sites lie within the Pacific Deep Water [*Fiedler and Talley*, 2006], so that the preferential preservation of opal at the sediment interface due to different bottom water conditions would have to involve changes over a large area. In addition, none of the environmental variables affecting the dissolution kinetics and solubility of biogenic opal (i.e., temperature, salinity, pH, pressure) could have changed significantly in bottom waters on the time scale of interest.

[37] On the other hand, two main mechanisms have been suggested to enhance opal preservation in the sediments.

[38] 1. *Sayles et al.* [2001] concluded that opal preservation is enhanced at higher sedimentation rates. However, we do not observe a significant change in sedimentation rate or in preserved bulk fluxes in our cores during the MIS3 peak as compared to the deglaciation peak (see Figure 2).

[39] 2. *Lewin* [1961] suggested that the incorporation of trace metals (Al, Be, Fe, Ga, Gd, Y) in diatomaceous opal during early diagenesis would lower its dissolution rate. *Van Bennekom et al.* [1991] have shown that both the dissolution rate and the equilibrium solubility of diatom silica decrease as the Al/Si ratio of the silica increases. Dissolved Al can be taken up by the deposited biogenic silica particles or it can form an aluminosilicate layer on the surface of the frustules within a few months [*Loucaides et al.*, 2010]. The extent and rate of this process appear to depend on the amount of Al available from coexisting detrital sediments. We have no trace element data for individual tests to verify this hypothesis.

[40] Other hypotheses related to the biomineralization of amorphous silica itself could lead to better preservation. The possible mechanisms for enhancing sedimentary preservation of biogenous opal in the EEP are as follows.

[41] 1. A shift in the diatom population occurs. The species composition of the diatom assemblage may play a major role in determining whether siliceous sediments accumulate on the seafloor. Different diatom species vary considerably in size, thickness, and specific surface area of their frustules. Most of the lightly silicified species appear to dissolve completely in the upper few hundred meters [*Gilbert and Allen*, 1943; *Litsitzin*, 1972]. *Gersonde and Wefer* [1987] found that differences in the relative abundance of diatom species between traps and surface sediments result from the disappearance of the less silicified diatom valves, leading to the enrichment of strongly silicified valves. Most of these changes seem to occur in the upper part of the water column, because the diatom associations found in the surface sediment more closely resemble those of deeper traps than the diatom assemblages in the surface waters [*Gersonde and Wefer*, 1987]. Dissolution transforms the initial diatom assemblage to an assemblage dominated by robust species [*Shemesh et al.*, 1989] and may alter the fraction of opal flux that is preserved [*Abelmann et al.*, 2006]. Smear slide observations on samples of ME-24 do not reveal significant changes in the diatom assemblage across the MIS3 event compared to core intervals above and below this event. There is thus no microfossil evidence to support species-driven changes in preserved opal.

[42] 2. There is a release from Si limitation. Si limitation can lower the Si:C ratio of diatoms by as much as a factor of 5 from that found in Si-replete cells [e.g., *Brzezinski*, 1992]. Diatoms do this by producing thinner frustules, making the cells much more susceptible to dissolution. A modest increase in the delivery of silicic acid as suggested by *Kienast et al.* [2006] for the EEP, could possibly decrease the Si limitation without having a large effect on production, which is also limited by other factors (e.g., grazing, iron supply) [*Leynaert et al.*, 2001].

[43] 3. There is an increase in Fe limitation. Studies report that Fe-limited diatoms grown in culture can have 1 to 2 times higher cellular Si:N biomass ratios as compared to Fe-replete diatoms [*Takeda*, 1998]. Thus, diatoms under Fe stress build frustules that are more heavily silicified [*Hutchins and Bruland*, 1998; *Takeda*, 1998]. From 35 to 60 kyr B.P., the EPICA Dome C ice core does indeed reveal very low atmospheric Fe (dust) flux (Figure 3d) [*Wolff et al.*, 2006].

[44] Because we are still unable to understand exactly what controls opal preservation in sediments today, it is difficult to interpret fully variations in opal preservation in the past. As shown here, a number of scenarios, non-mutually exclusive, could explain a better preservation of opal during the time of interest (MIS3). Drawing on mechanisms previously invoked in other locations or for different time intervals, we offer in the following a hypothesis on the most likely contributing factors to parsimoniously explain all our records.

5.4. High-Latitude Sea Ice and Low-Latitude Dust

[45] *Kienast et al.* [2006] assumed that higher opal production was responsible for the peak in opal deposition in the EEP during MIS3, and that silicic acid leakage from the Southern Ocean relieved EEP diatoms from Si limitation. This scenario follows the sea ice hypothesis [*Chase et al.*, 2003], which claims that excess silicic acid resulted from extended high-latitude sea ice cover, not from eolian-driven reduction in Si:N uptake ratio of diatoms as invoked in the original SALH. Silicon and nitrogen isotope records from the Indian sector of the Southern Ocean suggest low $Si(OH)_4$ utilization and strong NO_3 utilization during MIS2, and a reversed situation during the Holocene and MIS3 [*Crosta et al.*, 2005]. Thus, eolian-driven changes in nutrient dynamics of the Southern Ocean cannot cause the large deposition of opal in the EEP during MIS3, as the silicic acid content of intermediate waters during MIS3 was reduced compared to MIS2 [*Beucher et al.*, 2007].

[46] We therefore follow the sea ice scenario for silicic acid leakage during the last glacial period, but suggest that the lower atmospheric dust content during MIS3 plays a key role for opal deposition in the EEP. Increased high-latitude seasonal ice cover during the last glacial period (MIS 2–4, Figures 3d and 5) hampered diatom production and lessened silicic acid depletion in the Antarctic [*Anderson et al.*, 2002; *Chase et al.*, 2003; *Kohfeld et al.*, 2005; *Beucher et al.*, 2007], resulting in an enhanced delivery of $Si(OH)_4$ to the sub-Antarctic by Ekman flow. Antarctic sediments record this phenomenon by a northward shift of the zone of maximum diatom productivity ("the opal belt" (Figures 5b and 5c)). As a result, some unused Si was entrained in SAMW and exported to tropical upwelling areas. During MIS 2 and 4, increased dust supply to the Southern Ocean probably contributed to the sea ice effect by releasing diatoms from Fe stress and thus lowering their $Si(OH)_4$:NO_3 uptake ratios [*Matsumoto et al.*, 2002a; *Beucher et al.*, 2007]. Silicon isotope ratios from the sub-Antarctic suggest a reduced glacial Si utilization in the Southern Ocean, but this does not allow one to distinguish unequivocally between the sea ice-driven reduction in diatom productivity south of the Polar Front or local changes in nutrient uptake ratios driven by Fe [*Bradtmiller et al.*, 2009].

[47] *Pichevin et al.* [2009] recently suggested that enhanced glacial dust delivery affected the physiology of EEP diatoms in a similar way. Their EEP δ^{30}Si record shows lowered silicon utilization under iron-replete conditions during the LGM, thereby explaining the paradoxical decline in opal accumulation rate at that time. However, caution is required when interpreting silicon isotope ratios in the EEP, as they are influenced by several possible "upstream" effects that include (1) changes in Si utilization in source regions, (2) changes in the relative input of Si from major source regions (i.e., changes in relative input from the North Pacific and from the Southern Ocean), and (3) changes in the entrainment of Si from subtropical thermocline waters as subpolar waters transit toward the EUC formation region.

[48] In contrast to the situation during MIS2 and 4, Antarctic ice cores show that atmospheric dustiness was reduced during MIS3 (Figure 3d) [e.g., *Wolff et al.*, 2006]. A reduced dust flux during MIS3 is also inferred for the central and the eastern equatorial Pacific (Figure 3e) [*Winckler et al.*, 2008]. These authors used ^{230}Th-normalized ^{232}Th fluxes as a proxy for continental input, which at these locations is almost entirely driven by atmospheric deposition. The lower dustiness of MIS3 would have caused Fe limitation in the EEP, resulting in higher diatom $Si(OH)_4$:NO_3 uptake ratios and more heavily silicified frustules. As a consequence, the preservation of MIS3 diatom remains would be enhanced as compared to frustules built under the Fe-replete conditions of MIS2 and 4 (Figure 5).

[49] We note, however, that the EUC has been suggested as the primary source of Fe for the present-day equatorial upwelling system, through the interaction of the New Guinea Coastal Undercurrent (NGCUC) with Papua New Guinea (PNG) shelf sediments [*Gordon et al.*, 1997; *Wells et al.*, 1999; *Ryan et al.*, 2006]. The NGCUC intensification and shoaling observed during present-day El Niño events has been shown to increase the coupling of EUC to iron sources in PNG shelf sediments [*Ryan et al.*, 2006]. In contrast, lower glacial sea level along the PNG continental shelf would have deepened the NGCUC and thus hindered the entrainment of iron-bearing sediments from depositional zones on the shelf and upper slope. The delivery of PNG Fe to the EEP during MIS2–4 may have decreased to the point that eolian deposition would have become the critical source of Fe. The enhanced dustiness of MIS2 and 4 would have somewhat relieved the EEP from Fe limitation, whereas the lower dust flux of MIS3 would have contributed to the PNG-driven Fe limitation.

[50] The physiological basis for Fe effects on diatom silicon metabolism is poorly understood. In addition, another metal, zinc, may also be involved in diatom silicon metabolism [e.g., *Rueter and Morel*, 1981]. The effect of more heavily silicified frustules on metal-stressed cells may be a faster sinking rate for these cells than their nutrient-replete counterparts [e.g., *Muggli et al.*, 1996; *De La Rocha et al.*, 2000]. Rapid sinking of diatoms preserves a "seed population" of

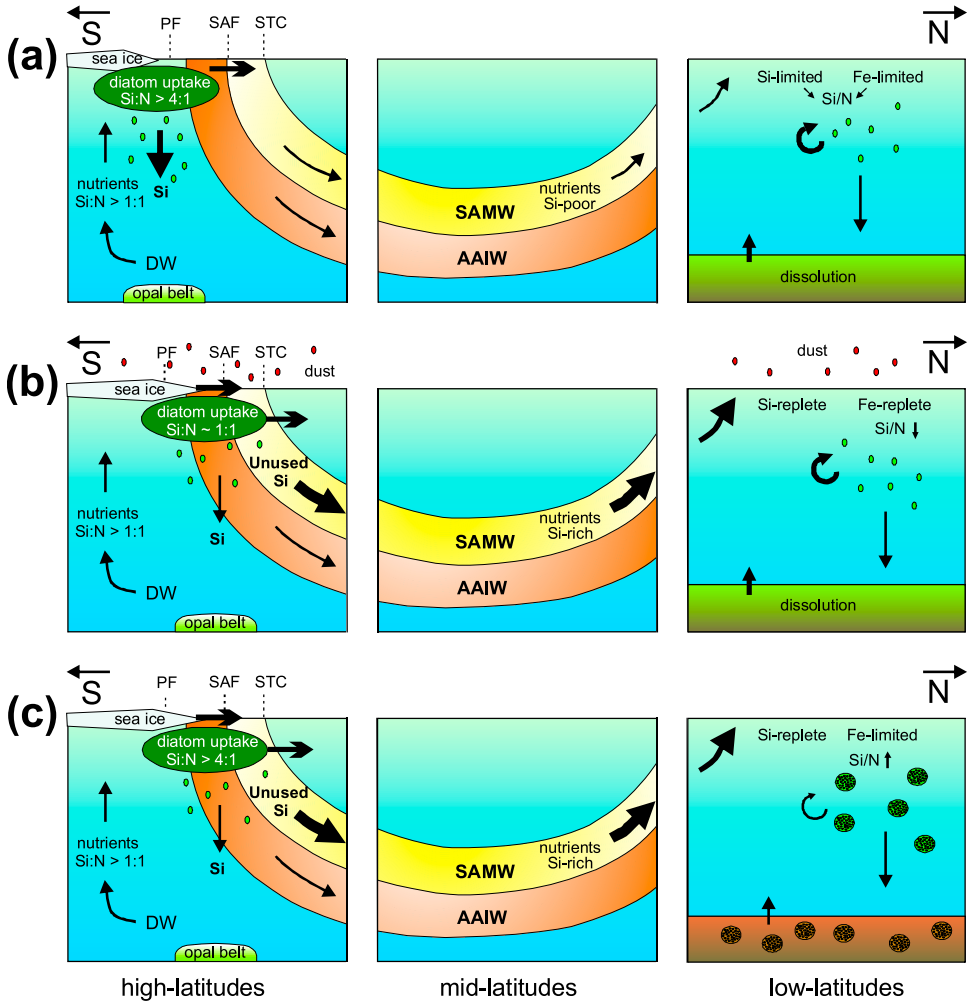

Figure 5. Schematic diagram of Subantarctic Mode Water (SAMW) circulation illustrating the various possible configurations of silicic acid supply from the Southern Ocean to the EEP upwelling environment. (a) Interglacial configuration. (b) Glacial configuration. (c) MIS3 configuration. PF stands for Polar Front, SAF stands for Subantarctic Front, STC stands for Subtropical Convergence Zone, DW stands for deep water, and AAIW stands for Antarctic Intermediate Water. Please refer to the text (section 5.4) for a complete description of the three scenarios.

cells in cool, dark, subsurface waters once surface conditions have become inhospitable to diatom growth [*Smetacek*, 1985], and is also a way to provide nutrient-stressed cells access to the more abundant nutrients at the depth of the subsurface nutricline [*Villareal et al.*, 1993; *Villareal and Carpenter*, 1994].

[51] It is noteworthy that the long-term opal record from core V19-28 (2°22′S 84°39′W, located between cores ME-24, ME-27 and TR-31) shows a peak of similar amplitude to the MIS3 peak around 280 kyr B.P. [*Lyle et al.*, 1988]. This earlier peak coincides with a prolonged interstadial (warm interval) at the beginning of MIS8. Similar conditions could be invoked for this older peak, i.e., low eolian Fe inputs, and higher Si leakage due to the presence of sea ice. Lower Fe and higher sea salt fluxes (the latter a proxy for winter sea ice extent) at EPICA Dome C in Antarctica are consistent with these inferred conditions [*Wolff et al.*, 2006].

[52] In summary, EEP sedimentary opal records seem to record both production and preservation events. We suggest that their relative importance changed over time, as a function of micronutrient and macronutrient supply. The Si- and Fe-replete conditions of the last glacial stage led to lowered Si utilization and diatom silicification, favoring dissolution of opal [*Pichevin et al.*, 2009], whereas the Si-replete and Fe-limited conditions of MIS3 enhanced the preservation of the diatom frustules. On the other hand, the peak in opal burial during the deglaciation can be clearly assigned to enhanced diatom productivity, as both brassicasterol and $(^{231}Pa/^{230}Th)_{xs,0}$ reveal coincident maxima. *Anderson et al.* [2009] attributed this deglacial opal peak to increased supply of nutrient-rich waters driven

by stronger upwelling of deep water in the Southern Ocean. Thus it seems that only very peculiar conditions as occurred during the deglaciation led to a clear productivity maximum.

[53] One approach to test the hypotheses suggested here would be to use microscopic studies of diatom remains in the sediments, in particular shell size, species composition and direct (morphological) assessment of valve preservation. *Warnock et al.* [2007] conducted such a study at ODP Site 846B (approximately 300 km south of the Galapagos Islands), which showed that there was no clear relationship between diatom preservation and opal accumulation during MIS1 and 2. Further work along these lines might be fruitful.

6. Conclusion

[54] We show that biogenic silica accumulation in the EEP not only reflects surface productivity. Our new $(^{231}Pa/^{230}Th)_{xs,0}$ ratio and brassicasterol concentration records imply that the large peak in opal deposition during MIS3 was not the result of enhanced diatom export production, as originally postulated by *Kienast et al.* [2006]. $(^{231}Pa/^{230}Th)_{xs,0}$ ratios are well correlated with opal fluxes during the last 23 kyr B.P., and they reveal a peak in opal export during the deglaciation that is also well defined in opal fluxes. However, during the larger opal peak interval (35–60 kyr B.P.), $(^{231}Pa/^{230}Th)_{xs,0}$ ratios and opal fluxes are decoupled, $(^{231}Pa/^{230}Th)_{xs,0}$ increasing slightly while opal fluxes more than triple. Because bulk fluxes do not show a significant increase over that interval, we suggest that the high opal fluxes result essentially from the higher opal content of the sediment. Since brassicasterol, an organic molecule commonly found in diatoms, also does not increase coeval with the opal peak, we suggest that the enhanced opal burial during that interval resulted from better preservation.

[55] Expanding on a scenario originally presented by *Kienast et al.* [2006], we suggest that the MIS3 "opal peak" results from a combination of silicic acid leakage from the high latitudes due to increased sea ice cover and low-dust/Fe conditions in the EEP. Thus, Fe limitation increased the Si/N consumption ratio by diatoms, leading to heavily silicified frustules, which improved their preservation in the sedimentary record. The interpretation presented here is consistent with the hypothesis of *Pichevin et al.* [2009], that enhanced atmospheric low-latitude dustiness during MIS2 and 4 can account for the absence of evidence for silicic acid leakage to lower latitudes during those two time intervals.

[56] In summary, our findings illustrate that both production (deglaciation) and preservation (MIS3) events are recorded in the sedimentary opal record of the EEP, and highlight the need for a multiproxy approach to differentiate between these two processes. Only after taking variable preservation of diatom frustules into account, can changes in EEP opal flux be used to test the predictions of the SALH hypothesis. This study also suggests that physiological responses of diatoms in the low-latitude ocean, often not considered in previous paleoceanographic studies, may be critically important in determining changes in opal flux preserved in the sedimentary record.

[57] **Acknowledgments.** Core material was kindly and generously provided by the Core Repositories of Oregon State University (supported by NSF grant OCE97-12024) and the University of Rhode Island (supported by NSF grant OCE-9102410) and the Lamont-Doherty Earth Observatory, Earth Institute at Columbia University. We gratefully acknowledge Christelle Not and Maureen Soon for their help with Pa/Th laboratory work, Mysti Weber for her smear slide investigations, Alan Mix for the sharing of unpublished age models, and an anonymous reviewer for his/her constructive comments. This work was supported by NSERC Canada (M.K., S.K., S.E.C., and R.F.), NSF (R.F.A.), the Canadian Institute for Advanced Research (M.K.), the Canadian Foundation for Climate and Atmospheric Sciences (S.E.C. and R.F.) and the International Association of Sedimentologists (N.D.).

References

Abelmann, A., R. Gersonde, G. Cortese, G. Kuhn, and V. Smetacek (2006), Extensive phytoplankton blooms in the Atlantic sector of the glacial Southern Ocean, *Paleoceanography*, *21*, PA1013, doi:10.1029/2005PA001199.

Anderson, R. F., M. P. Bacon, and P. G. Brewer (1983), Removal of ^{230}Th and ^{231}Pa at ocean margins, *Earth Planet. Sci. Lett.*, *66*, 73–90, doi:10.1016/0012-821X(83)90127-9.

Anderson, R. F., Y. Lao, W. S. Broecker, S. E. Trumbore, H. J. Hofmann, and W. Wolfli (1990), Boundary scavenging in the Pacific Ocean: A comparison of ^{10}Be and ^{231}Pa, *Earth Planet. Sci. Lett.*, *96*, 287–304, doi:10.1016/0012-821X(90)90008-L.

Anderson, R. F., Z. Chase, M. Q. Fleisher, and J. P. Sachs (2002), The Southern Ocean's biological pump during the Last Glacial Maximum, *Deep Sea Res., Part II*, *49*, 1909–1938, doi:10.1016/S0967-0645(02)00018-8.

Anderson, R. F., S. Ali, L. I. Bradtmiller, S. H. H. Nielsen, M. Q. Fleisher, B. E. Anderson, and L. H. Burckle (2009), Wind-driven upwelling in the Southern Ocean and the deglacial rise in atmospheric CO_2, *Science*, *323*, 1443–1448, doi:10.1126/science.1167441.

Antoine, D., J.-M. André, and A. Morel (1996), Oceanic primary production: 2. Estimation at global scale from satellite (coastal zone color scanner) chlorophyll, *Global Biogeochem. Cycles*, *10*, 57–69, doi:10.1029/95GB02832.

Archer, D., M. Lyle, K. Rodgers, and P. Froelich (1993), What controls opal preservation in tropical deep-sea sediments?, *Paleoceanography*, *8*, 7–21, doi:10.1029/92PA02803.

Beucher, C. P., M. A. Brzezinski, and X. Crosta (2007), Silicic acid dynamics in the glacial sub-Antarctic: Implications for the silicic acid leakage hypothesis, *Global Biogeochem. Cycles*, *21*, GB3015, doi:10.1029/2006GB002746.

Boyle, E. A. (1983), Chemical accumulation variations under the Peru Current during the past 130,000 years, *J. Geophys. Res.*, *88*(C12), 7667–7680, doi:10.1029/JC088iC12p07667.

Bradtmiller, L. I., R. F. Anderson, M. Q. Fleisher, and L. H. Burckle (2006), Diatom productivity in the equatorial Pacific Ocean from the last glacial period to the present: A test of the silicic acid leakage hypothesis, *Paleoceanography*, *21*, PA4201, doi:10.1029/2006PA001282.

Bradtmiller, L. I., R. F. Anderson, M. Q. Fleisher, and L. H. Burckle (2007), Opal burial in the equatorial Atlantic Ocean over the last 30 ka: Implications for glacial-interglacial changes in the ocean silicon cycle, *Paleoceanography*, *22*, PA4216, doi:10.1029/2007PA001443.

Bradtmiller, L. I., R. F. Anderson, M. Q. Fleisher, and L. H. Burckle (2009), Comparing glacial and Holocene opal fluxes in the Pacific sector of the Southern Ocean, *Paleoceanography*, *24*, PA2214, doi:10.1029/2008PA001693.

Brzezinski, M. A. (1992), Cell-cycle effects on the kinetics of silicic acid uptake and resource competition among diatoms, *J. Plankton Res.*, *14*, 1511–1539, doi:10.1093/plankt/14.11.1511.

Brzezinski, M. A., C. J. Pride, V. M. Frank, D. M. Sigman, J. L. Sarmiento, K. Matsumoto, N. Gruber, G. H. Rau, and K. H. Coale (2002), A switch from $Si(OH)_4$ to NO_3^- depletion in the glacial Southern Ocean, *Geophys. Res. Lett.*, *29*(12), 1564, doi:10.1029/2001GL014349.

Calvo, E., C. Pelejero, G. A. Logan, and P. De Dekker (2004), Dust-induced changes in phytoplankton composition in the Tasman Sea during the last four glacial cycles, *Paleoceanography*, *19*, PA2020, doi:10.1029/2003PA000992.

Charles, C. D., P. N. Froehlich, M. A. Zibello, R. A. Mortlock, and J. J. Morley (1991), Biogenic opal in Southern Ocean sediments over the last 450,000 years: Implications for surface water chemistry and circulation, *Paleoceanography*, *6*, 697–728, doi:10.1029/91PA02477.

Chase, Z., R. F. Anderson, M. Q. Fleisher, and P. W. Kubik (2002), The influence of particle composition and particle flux on scavenging of Th, Pa and Be in the ocean, *Earth Planet. Sci. Lett.*, *204*, 215–229, doi:10.1016/S0012-821X(02)00984-6.

Chase, Z., R. F. Anderson, M. Q. Fleisher, and P. W. Kubik (2003), Accumulation of biogenic and lithogenic material in the Pacific sector of the Southern Ocean during the past 40,000 years, *Deep Sea Res., Part II*, *50*, 799–832, doi:10.1016/S0967-0645(02)00595-7.

Chavez, F. P., K. R. Buck, and R. T. Barber (1990), Phytoplankton taxa in relation to primary production in the equatorial Pacific, *Deep Sea Res., Part A*, *37*, 1733–1752, doi:10.1016/0198-0149(90)90074-6.

Choi, M. S., R. Francois, K. Sims, M. P. Bacon, S. Brown-Leger, A. P. Fleer, L. Ball, D. Schneider, and S. Pichat (2001), Rapid determination of ^{230}Th and ^{231}Pa in seawater by desolvated micro-nebulization inductively coupled plasma magnetic sector mass spectrometry, *Mar. Chem.*, *76*, 99–112, doi:10.1016/S0304-4203(01)00050-0.

Conte, M. H., J. K. Volkman, and G. Eglinton (1994), Lipid biomarkers of the Haptophyta, in *The Haptophyte Algae*, edited by J. C. Green and B. S. C. Leadbetter, pp. 351–377, Clarendon Univ. Press, Oxford, U. K.

Crosta, X., A. Sturm, L. Armand, and J.-J. Pichon (2004), Late Quaternary sea ice history in the Indian sector of the Southern Ocean as recorded by diatom assemblages, *Mar. Micropaleontol.*, *50*, 209–223, doi:10.1016/S0377-8398(03)00072-0.

Crosta, X., A. Shemesh, J. Etourneau, R. Yam, I. Billy, and J. J. Pichon (2005), Nutrient cycling in the Indian sector of the Southern Ocean over the last 50,000 years, *Global Biogeochem. Cycles*, *19*, GB3007, doi:10.1029/2004GB002344.

Crosta, X., C. Beucher, K. Pahnke, and M. A. Brzezinski (2007), Silicic acid leakage from the Southern Ocean: Opposing effects of nutrient uptake and oceanic circulation, *Geophys. Res. Lett.*, *34*, L13601, doi:10.1029/2006GL029083.

De La Rocha, C. L., M. A. Brzezinski, M. J. DeNiro, and A. Shemesh (1998), Silicon-isotope composition of diatoms as an indicator of past oceanic change, *Nature*, *395*, 680–683, doi:10.1038/27174.

De La Rocha, C. L., D. A. Hutchins, M. A. Brzezinski, and Y. Zhang (2000), Effects of iron and zinc deficiency on elemental composition and silica production by diatoms, *Mar. Ecol. Prog. Ser.*, *195*, 71–79, doi:10.3354/meps195071.

Dezileau, L., G. Bareille, and J. L. Reyss (2003), The ^{231}Pa/^{230}Th ratio as a proxy for past changes in opal fluxes in the Indian sector of the Southern Ocean, *Mar. Chem.*, *81*, 105–117, doi:10.1016/S0304-4203(02)00070-1.

Dugdale, R. C., and F. P. Wilkerson (1998), Silicate regulation of new production in the equatorial Pacific upwelling, *Nature*, *391*, 270–273, doi:10.1038/34630.

Dugdale, R. C., F. P. Wilkerson, and H. J. Minas (1995), The role of a silicate pump in driving new production, *Deep Sea Res., Part I*, *42*, 697–719, doi:10.1016/0967-0637(95)00015-X.

Dugdale, R. C., A. G. Wischmeyer, F. P. Wilkerson, R. T. Barber, F. Chai, M.-S. Jiang, and T.-H. Peng (2002), Meridional asymmetry of source nutrients to the equatorial Pacific upwelling ecosystem and its potential impact on ocean-atmosphere CO_2 flux: A data and modeling approach, *Deep Sea Res., Part II*, *49*, 2513–2531, doi:10.1016/S0967-0645(02)00046-2.

Fiedler, P. C., and L. D. Talley (2006), Hydrography of the eastern tropical Pacific: A review, *Prog. Oceanogr.*, *69*, 143–180, doi:10.1016/j.pocean.2006.03.008.

Franck, V. M., G. J. Smith, K. W. Bruland, and M. A. Brzezinski (2005), Comparison of size-dependent carbon, nitrate, and silicic acid uptake rates in high- and low-iron waters, *Limnol. Oceanogr.*, *50*, 825–838, doi:10.4319/lo.2005.50.3.0825.

Francois, R., M. Frank, M. M. Rutgers van der Loeff, and M. P. Bacon (2004), ^{230}Th normalization: An essential tool for interpreting sedimentary fluxes during the late Quaternary, *Paleoceanography*, *19*, PA1018, doi:10.1029/2003PA000939.

Garcia, H. E., R. A. Locarnini, T. P. Boyer, and J. I. Antonov (2006), *World Ocean Atlas 2005*, vol. 4, *Nutrients (Phosphate, Nitrate, and Silicate)*, *NOAA Atlas NESDIS*, vol. 64, edited by S. Levitus, 396 pp., NOAA, Silver Spring, Md.

Gersonde, R., and G. Wefer (1987), Sedimentation of biogenic siliceous particles in Antarctic waters from the Atlantic sector, *Mar. Micropaleontol.*, *11*, 311–332, doi:10.1016/0377-8398(87)90004-1.

Gilbert, J. Y., and W. E. Allen (1943), The phytoplankton of the Gulf of California obtained by the "E.W. Scripps" in 1939 and 1940, *J. Mar. Res.*, *5*, 89–110.

Gordon, R. M., K. H. Coale, and K. S. Johnson (1997), Iron distributions in the equatorial Pacific: Implications for new production, *Limnol. Oceanogr.*, *42*, 419–431, doi:10.4319/lo.1997.42.3.0419.

Harrison, K. G. (2000), Role of increased marine silica input on paleo-pCO_2 levels, *Paleoceanography*, *15*, 292–298, doi:10.1029/1999PA000427.

Higginson, M. J., and M. A. Altabet (2004), Initial test of the silicic acid leakage hypothesis using sedimentary biomarkers, *Geophys. Res. Lett.*, *31*, L18303, doi:10.1029/2004GL020511.

Hiscock, M. R., J. Marra, W. O. Smith Jr., R. Goericke, C. Measures, S. Vink, R. J. Olson, H. M. Sosik, and R. T. Barber (2003), Primary productivity and its regulation in the Pacific sector of the Southern Ocean, *Deep Sea Res., Part II*, *50*, 533–558, doi:10.1016/S0967-0645(02)00583-0.

Hutchins, D. A., and K. W. Bruland (1998), Iron-limited diatom growth and Si:N uptake ratios in a coastal upwelling regime, *Nature*, *393*, 561–564, doi:10.1038/31203.

Kamatani, A., N. Ejiri, and P. Tréguer (1988), The dissolution kinetics of diatom ooze from the Antarctic area, *Deep Sea Res., Part A*, *35*, 1195–1203, doi:10.1016/0198-0149(88)90010-6.

Kienast, S. S., M. Kienast, S. Jaccard, S. E. Calvert, and R. François (2006), Testing the silica leakage hypothesis with sedimentary opal records from the eastern equatorial Pacific over the last 150 kyrs, *Geophys. Res. Lett.*, *33*, L15607, doi:10.1029/2006GL026651.

Kienast, S. S., M. Kienast, A. C. Mix, S. E. Calvert, and R. François (2007), Thorium-230 normalized particle flux and sediment focusing in the Panama Basin region during the last 30,000 years, *Paleoceanography*, *22*, PA2213, doi:10.1029/2006PA001357.

Kohfeld, K. E., C. Le Quere, S. P. Harrison, and R. F. Anderson (2005), Role of marine biology in glacial-interglacial CO_2 cycles, *Science*, *308*, 74–78, doi:10.1126/science.1105375.

Ku, T.-L., S. Luo, M. Kusakabe, and J. K. B. Bishop (1995), ^{228}Ra-derived nutrient budgets in the upper equatorial Pacific and the role of "new" silicate in limiting productivity, *Deep Sea Res., Part II*, *42*, 479–497, doi:10.1016/0967-0645(95)00020-Q.

Kusch, S., T. I. Eglinton, A. C. Mix, and G. Mollenhauer (2010), Timescales of lateral sediment transport in the Panama Basin as revealed by radiocarbon ages of alkenones, total organic carbon and foraminifera, *Earth Planet. Sci. Lett.*, *290*, 340–350, doi:10.1016/j.epsl.2009.12.030.

Lange, C. B., and W. H. Berger (1993), Diatom productivity and preservation in the western equatorial Pacific: The Quaternary record, *Proc. Ocean Drill. Program Sci. Results*, *130*, 509–523.

Lea, D. W., D. K. Pak, C. L. Belanger, H. J. Spero, M. A. Hall, and N. J. Shackleton (2006), Paleoclimate history of Galapagos surface waters over the last 135,000 yr, *Quat. Sci. Rev.*, *25*, 1152–1167, doi:10.1016/j.quascirev.2005.11.010.

Leinen, M., D. Cwienk, G. R. Heath, P. E. Biscaye, V. Kolla, J. Thiede, and J. P. Dauphin (1986), Distribution of biogenic silica and quartz in recent deep-sea sediments, *Geology*, *14*, 199–203, doi:10.1130/0091-7613(1986)14<199:DOBSAQ>2.0.CO;2.

Lewin, J. C. (1961), The dissolution of silica from diatom walls, *Geochim. Cosmochim. Acta*, *21*, 182–196, doi:10.1016/S0016-7037(61)80054-9.

Leynaert, A., P. Tréguer, C. Lancelot, and M. Rodier (2001), Silicon limitation of biogenic silica production in the equatorial Pacific, *Deep Sea Res., Part I*, *48*, 639–660, doi:10.1016/S0967-0637(00)00044-3.

Litsitzin, A. P. (1972), Sedimentation in the world ocean, *Spec. Publ. Soc. Econ. Paleontol. Mineral.*, *17*, 218–241.

Loucaides, S., P. Michalopoulos, M. Presti, E. Koning, T. Behrends, and P. Van Cappellen (2010), Seawater-mediated interactions between diatomaceous silica and terrigenous sediments: Results from long-term incubation experiments, *Chem. Geol.*, *270*, 68–79, doi:10.1016/j.chemgeo.2009.11.006.

Lyle, M., D. W. Murray, B. P. Finney, J. Dymond, J. M. Robbins, and K. Brooksforce (1988), The record of Late Pleistocene biogenic sedimentation in the eastern tropical Pacific Ocean, *Paleoceanography*, *3*, 39–59, doi:10.1029/PA003i001p00039.

Lyle, M., N. Mitchell, N. Pisias, A. Mix, J. I. Martinez, and A. Paytan (2005), Do geochemical estimates of sediment focusing pass the sediment test in the equatorial Pacific?, *Paleoceanography*, *20*, PA1005, doi:10.1029/2004PA001019.

Matsumoto, K., and J. Lynch-Stieglitz (1999), Similar glacial and Holocene deep water circulation inferred from southeast Pacific benthic fora-

miniferal carbon isotope composition, *Paleoceanography*, *14*, 149–163, doi:10.1029/1998PA900028.

Matsumoto, K., and J. L. Sarmiento (2008), A corollary to the silicic acid leakage hypothesis, *Paleoceanography*, *23*, PA2203, doi:10.1029/2007PA001515.

Matsumoto, K., J. L. Sarmiento, and M. A. Brzezinski (2002a), Silicic acid leakage from the Southern Ocean: A possible explanation for glacial atmospheric pCO_2, *Global Biogeochem. Cycles*, *16*(3), 1031, doi:10.1029/2001GB001442.

Matsumoto, K., T. Oba, J. Lynch-Stieglitz, and H. Yamamoto (2002b), Interior hydrography and circulation of the glacial Pacific Ocean, *Quat. Sci. Rev.*, *21*, 1693–1704, doi:10.1016/S0277-3791(01)00142-1.

Minas, H. J., M. Minas, and T. T. Packard (1986), Productivity in upwelling areas deduced from hydrographic and chemical fields, *Limnol. Oceanogr.*, *31*, 1182–1206, doi:10.4319/lo.1986.31.6.1182.

Moore, T. C., G. R. Heath, and R. O. Kowsmann (1973), Biogenic sediments of the Panama Basin, *J. Geol.*, *81*, 458–472, doi:10.1086/627884.

Mortlock, R. A., and P. N. Froelich (1989), A simple method for the rapid determination of biogenic opal in pelagic marine sediments, *Deep Sea Res., Part A*, *36*, 1415–1426, doi:10.1016/0198-0149(89)90092-7.

Muggli, D. L., M. Lecourt, and P. J. Harrison (1996), Effects of iron and nitrogen source on the sinking rate, physiology and metal composition of an oceanic diatom from the subarctic Pacific, *Mar. Ecol. Prog. Ser.*, *132*, 215–227, doi:10.3354/meps132215.

Murray, D. W. (1987), Spatial and temporal variations in sediment accumulation in the central tropical Pacific, Ph.D. thesis, 343 pp., Oregon State Univ., Corvallis.

Nelson, D. M., P. Tréguer, M. A. Brzezinski, A. Leynaert, and B. Quéguiner (1995), Production and dissolution of biogenic silica in the ocean: Revised global estimates, comparison with regional data and relationship to biogenic sedimentation, *Global Biogeochem. Cycles*, *9*, 359–372, doi:10.1029/95GB01070.

Nozaki, Y., and T. Oba (1995), Dissolution of calcareous tests in the ocean and atmospheric carbon dioxide, in *Biogeochemical Processes and Ocean Fluxes in the Western Pacific*, edited by H. Sakai and Y. Nozaki, pp. 83–92, Terra Sci., Tokyo.

Nozaki, Y., and Y. Yamamoto (2001), Radium 228 based nitrate fluxes in the eastern Indian Ocean and the South China Sea and a silicon-induced "alkalinity pump" hypothesis, *Global Biogeochem. Cycles*, *15*, 555–567, doi:10.1029/2000GB001309.

Pichat, S., K. W. W. Sims, R. François, J. F. McManus, S. Brown Leger, and F. Albarède (2004), Lower export production during glacial periods in the equatorial Pacific derived from $(^{231}Pa/^{230}Th)_{xs,0}$ measurements in deep-sea sediments, *Paleoceanography*, *19*, PA4023, doi:10.1029/2003PA000994.

Pichevin, L. E., B. C. Reynolds, R. S. Ganeshram, I. Cacho, L. D. Pena, K. Keefe, and R. M. Ellam (2009), Enhanced carbon pump inferred from relaxation of nutrient limitation in the glacial ocean, *Nature*, *459*, 1114–1117, doi:10.1038/nature08101.

Pichon, J. J., G. Bareille, M. Labracherie, L. D. Labeyrie, A. Baudrimont, and J. L. Turon (1992), Quantification of the biogenic silica dissolution in Southern Ocean sediments, *Quat. Res.*, *37*, 361–378, doi:10.1016/0033-5894(92)90073-R.

Ragueneau, O., et al. (2000), A review of the Si cycle in the modern ocean: Recent progress and missing gaps in the application of biogenic opal as a paleoproductivity proxy, *Global Planet. Change*, *26*, 317–365, doi:10.1016/S0921-8181(00)00052-7.

Rampen, S. W., B. A. Abbas, S. Schouten, and J. S. Sinninghe Damsté (2010), A comprehensive study of sterols in marine diatoms (Bacillariophyta): Implications for their use as tracers for diatom productivity, *Limnol. Oceanogr.*, *55*, 91–105.

Richaud, M., P. Loubere, S. Pichat, and R. Francois (2007), Changes in opal flux and the rain ratio during the last 50,000 years in the equatorial Pacific, *Deep Sea Res., Part II*, *54*, 762–771, doi:10.1016/j.dsr2.2007.01.012.

Romero, O. E., C. B. Lange, G. Fisher, U. F. Treppke, and G. Wefer (1999), Variability in export production documented by downward fluxes and species composition of marine planktic diatoms: Observations from the tropical and equatorial Atlantic, in *Use of Proxies in Paleoceanography: Examples From the South Atlantic*, edited by G. Fischer and G. Wefer, pp. 365–392, Springer, Berlin.

Rueter, J. G., Jr., and F. M. M. Morel (1981), The interaction between zinc deficiency and copper toxicity as it affects silicic acid uptake mechanisms in *Thalassiosira pseudonana*, *Limnol. Oceanogr.*, *26*, 67–73, doi:10.4319/lo.1981.26.1.0067.

Ryan, J. P., I. Ueki, Y. Chao, H. Zhang, P. S. Polito, and F. P. Chavez (2006), Western Pacific modulation of large phytoplankton blooms in the central and eastern equatorial Pacific, *J. Geophys. Res.*, *111*, G02013, doi:10.1029/2005JG000084.

Sachs, J. P., and R. F. Anderson (2005), Increased productivity in the subantarctic ocean during Heinrich events, *Nature*, *434*, 1118–1121, doi:10.1038/nature03544.

Sancetta, C. (1992), Comparison of phytoplankton in sediment trap time series and surface sediments along a productivity gradient, *Paleoceanography*, *7*, 183–194, doi:10.1029/92PA00156.

Sarmiento, J. L., N. Gruber, M. A. Brzezinski, and J. P. Dunne (2004), High-latitude controls of thermocline nutrients and low latitude biological productivity, *Nature*, *427*, 56–60, doi:10.1038/nature02127.

Sayles, F. L., W. R. Martin, Z. Chase, and R. F. Anderson (2001), Benthic remineralization and burial of biogenic SiO_2, $CaCO_3$, organic carbon, and detrital material in the Southern Ocean along a transect at 170° west, *Deep Sea Res., Part II*, *48*, 4323–4383, doi:10.1016/S0967-0645(01)00091-1.

Schneider, R. R., B. Price, P. J. Müller, D. Kroon, and I. Alexander (1997), Monsoon related variations in Zaire (Congo) sediment load and influence of fluvial silicate supply on marine productivity in the east equatorial Atlantic during the last 200,000 years, *Paleoceanography*, *12*, 463–481, doi:10.1029/96PA03640.

Schubert, C. J., J. Villanueva, S. E. Calvert, G. L. Cowie, U. Von Rad, H. Schulz, U. Berner, and H. Erlenkeuser (1998), Stable phytoplankton community structure in the Arabian Sea over the past 200,000 years, *Nature*, *394*, 563–566, doi:10.1038/29047.

Shackleton, N. J., M. A. Hall, J. Line, and C. Shuxi (1983), Carbon isotope data in core V19-30 confirm reduced carbon dioxide concentration in the ice age atmosphere, *Nature*, *306*, 319–322, doi:10.1038/306319a0.

Shemesh, A., L. H. Burckle, and P. N. Froelich (1989), Dissolution and preservation of Antarctic diatoms and the effect on sediment thanatocoenoses, *Quat. Res.*, *31*, 288–308, doi:10.1016/0033-5894(89)90010-0.

Smetacek, V. S. (1985), Role of sinking in diatom life-history cycles: Ecological, evolutionary and geological significance, *Mar. Biol. Berlin*, *84*, 239–251, doi:10.1007/BF00392493.

Smith, W. H. F., and D. T. Sandwell (1997), Global sea floor topography from satellite altimetry and ship depth soundings, *Science*, *277*, 1956–1962, doi:10.1126/science.277.5334.1956.

Stumm, W., and J. J. Morgan (1981), *Aquatic Chemistry*, 2nd ed., 780 pp., John Wiley, New York.

Takeda, S. (1998), Influence of iron availability on nutrient consumption ratio of diatoms in oceanic waters, *Nature*, *393*, 774–777, doi:10.1038/31674.

Tande, K. S., and D. Slagstad (1985), Assimilation efficiency in herbivorous aquatic organisms—The potential of the ratio methods using ^{14}C and biogenic silica as markers, *Limnol. Oceanogr.*, *30*, 1093–1099, doi:10.4319/lo.1985.30.5.1093.

Toggweiler, J. R., K. Dixon, and W. S. Broecker (1991), The Peru upwelling and the ventilation of the South Pacific thermocline, *J. Geophys. Res.*, *96*(C11), 20,467–20,497, doi:10.1029/91JC02063.

Van Andel, T. H. (1973), Texture and dispersal of sediments in the Panama Basin, *J. Geol.*, *81*, 434–457, doi:10.1086/627883.

Van Bennekom, A. J., A. G. J. Buma, and R. F. Nolting (1991), Dissolved aluminium in the Weddell-Scotia Confluence and effect of Al on the dissolution kinetics of biogenic silica, *Mar. Chem.*, *35*, 423–434, doi:10.1016/S0304-4203(09)90034-2.

Villareal, T. A., and E. J. Carpenter (1994), Chemical composition and photosynthetic characteristics of *Ethmodiscus rex* (Bacillariophyceae): Evidence for vertical migration, *J. Phycol.*, *30*, l–8, doi:10.1111/j.0022-3646.1994.00001.x.

Villareal, T. A., M. A. Altabet, and K. Culver-Rymsza (1993), Nitrogen transport by vertically migrating diatom mats in the North Pacific Ocean, *Nature*, *363*, 709–712, doi:10.1038/363709a0.

Volkman, J. K. (1986), A review of sterol markers for marine and terrigenous organic matter, *Org. Geochem.*, *9*(2), 83–99, doi:10.1016/0146-6380(86)90089-6.

Volkman, J. K. (2003), Sterols in microorganisms, *Appl. Microbiol. Biotechnol.*, *60*, 495–506.

Warnock, J., R. Scherer, and P. Loubere (2007), A quantitative assessment of diatom dissolution and late Quaternary primary productivity in the eastern equatorial Pacific, *Deep Sea Res., Part II*, *54*, 772–783, doi:10.1016/j.dsr2.2007.01.011.

Wefer, G., W. H. Berger, J. Bijma, and G. Fischer (1999), Clues to ocean history: A brief overview of proxies, in *Use of Proxies in Paleoceano-*

graphy: Examples From the South Atlantic, edited by G. Fischer and G. Wefer, pp. 1–68, Springer, Berlin.

Wells, M. L., G. K. Vallis, and E. A. Silver (1999), Tectonic processes in Papua New Guinea and past productivity in the eastern equatorial Pacific Ocean, *Nature*, *398*, 601–604, doi:10.1038/19281.

Winckler, G., R. F. Anderson, M. Q. Fleisher, D. McGee, and N. Mahowald (2008), Covariant glacial-interglacial dust fluxes in the equatorial Pacific and Antarctica, *Science*, *320*, 93–96, doi:10.1126/science.1150595.

Wolff, E. W., et al. (2006), Southern Ocean sea-ice extent, productivity and iron flux over the past eight glacial cycles, *Nature*, *440*, 491–496, doi:10.1038/nature04614.

R. F. Anderson, Lamont-Doherty Earth Observatory, Earth Institute at Columbia University, Palisades, NY 10964, USA.

S. E. Calvert and R. François, Department of Earth and Ocean Sciences, University of British Columbia, Vancouver, BC V6T 1Z4, Canada.

N. Dubois, M. Kienast, and S. Kienast, Department of Oceanography, Dalhousie University, Halifax, NS B3H 4J1, Canada. (nathalie.dubois@dal.ca)